ISSN (Print) 1226-1750
ISSN (Online) 2233-6656
Journal of Magnetics 24(1), 1-9 (2019) https://doi.org/10.4283/JMAG.2019.24.1.001

Direct Calculation Method of Fringing Field Reluctance in MEC Analysis for An Axisymmetric Solenoid Actuator

Yong-Suk Hwang and Jung-Pyo Hong*

Department of Automotive Engineering, Hanyang University, Seoul 04763, Korea

(Received 12 October 2018, Received in final form 25 January 2019, Accepted 26 January 2019)

In this paper, a method is introduced to directly calculate the reluctances of fringing fields in analyzing a magnetic equivalent circuit model for an axisymmetric solenoid actuator including radial air gaps as well as axial air gaps. The introduced method was motivated by the possibility to calculate the cross section area depending on the radial position of an infinitesimal element when the infinitesimal element is defined to be integrated in the flux flow direction in a circular-arc straight-line model of an axisymmetric model. In this method, the reluctance of fringing field near an air gap can be calculated directly. For an objective model, the MEC analysis was performed using the introduced method and an iterative method. In the iterative method, the nonlinearity of the ferromagnetic material parts is resolved. In order to validate the introduced method, MEC analysis and FEA results are compared. And for validating the method in a view of computation also, an optimized design satisfying pre-defined constraints was searched using MEC analysis, and then the results of the MEC analysis using the introduced method and FEA results are compared for the searched design and the initial design.

Keywords : magnetic equivalent circuit, fringing effect, axisymmetric solenoid actuator, direct reluctance calculation

1. Introduction

The Magnetic Equivalent Circuit (MEC) model has been being used widely for analyses of electromagnetic devices since the late 19th century when Rowland presented the idea for a magnetic flux law [1] and still now [2-5]. The accuracy of MEC analysis may be a drawback compared to the Finite Element Analysis (FEA) but MEC analysis is still useful because of the cheap cost in computation. Especially, MEC analysis is very useful in the initial design stage because the initial design is chosen among a lot of combinations of several design parameters varying in a range. And the flux path of solenoid actuator is clearer than other type of electromagnetic devices so an acceptable accuracy can be obtained from MEC analysis. Additionally, improved methods of the MEC analyses are being proposed continuously as in [4] and [5] so that the accuracy of the analysis is getting higher.

However, a method has not been suggested to calculate the fringing effect near a radial air gap in an axisymmetric model and to have an acceptable accuracy, although the axisymmetric is widely used shape and the radial air gap is included in several application cases. The fringing effects near air gaps were considered in [4] but it was only for the planar model stacked enough in normal direction of a plane. The MEC for an axisymmetric model was configured in [5] but a method was not presented to consider the fringing effect near a radial air gap. The fringing effect near a radial air gap was considered graphically in [2], but as it was presented in [5], the accuracy is not enough. A circular-arc straight-line model has been introduced in [9] for considering fringing effect near an air gap between ferromagnetic material. And the model was used in [4] and [5]. In an axisymmetric model, if an infinitesimal element is defined as like in [4], [5] and [9], complex multiple integral problem occurs when the area and length of the infinitesimal element are substituted to (1) or (2) in order to calculate reluctance or permeance. Reluctance is defined as (1) and permeance is the reciprocal of reluctance as (2) [6].

$$R = \frac{l}{\mu S} \tag{1}$$

where,

R : Reluctance [H^{-1}]

*Corresponding author: Tel: +82-2-2220-4466
Fax: +82-2-2220-4465, e-mail: hongjp@hanyang.ac.kr

l : the length of flux path [m]
μ : the absolute permeability [H/m]
S : the cross section area of flux path [m^2]

$$P = \frac{1}{R} \tag{2}$$

where,

P : Permeance [H]

In [5], in order to avoid this kind of mathematical difficulty, a reference radius and an effective length were introduced and the permeance of fringing field was calculated using them. But there was no solution to calculate the fringing effect near radial air gap as mentioned before.

In this paper, a method is introduced to directly calculate the reluctances of fringing fields in analyzing a magnetic equivalent circuit model for an axisymmetric solenoid actuator including radial air gaps as well as axial air gaps. The introduced method was motivated by the possibility to calculate the cross section area depending on the radial position of an infinitesimal element when the infinitesimal element is defined to be integrated in the flux flow direction in a circular-arc straight-line model of an axisymmetric model. In this method, the reluctance of fringing field near an air gap can be calculated directly. For an objective model, the MEC analysis was performed using the introduced method and an iterative method. In the iterative method, the nonlinearity of the ferromagnetic material parts is resolved. In order to validate the introduced method, MEC analysis and FEA result are compared. And for validating the method in a view of computation also, an optimized design satisfying pre-defined constraints was searched using MEC analysis, and then the results of the MEC analysis using the introduced method and FEA results are compared for the searched design and the initial design.

2. Direct Reluctance Calculations of Air Gaps and Fringing Fields

As mentioned before, in this paper the circular-arc straight-line model [9] was applied for considering the fringing field near air gap.

It is shown in Fig. 1 the outer fringing field of an axial air gap for an axisymmetric solenoid actuator. The fringing field consists of two quadrants and a rectangle. The X_1 determines the range of fringing field. And it is set manually and empirically as mentioned in [9]. In Fig. 1, only one side of quadrants and a rectangle are presented for avoiding complexity. The reluctance dR_{quad1} of the infinitesimal element in the presented quadrant can be formulated as (3) referring to (1).

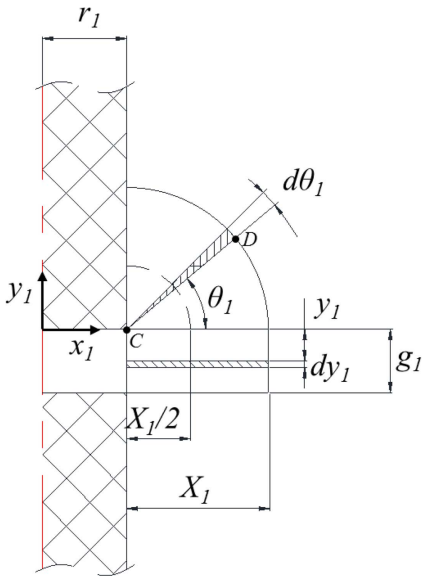

Fig. 1. (Color online) The outer fringing field of axial air gap.

$$dR_{quad1} = \frac{dl_{quad1}}{\mu_0 S_{\theta_1}} \tag{3}$$

where,

dR_{quad1}: the reluctance of the infinitesimal element
dl_{quad1} : the length of flux path
μ_0 : the permeability of vacuum.
S_{θ_1} : the cross section area which flux flows.

For the infinitesimal element in Fig. 1, the length of flux path dl_{quad1} can be expressed as a mean length of flux path as (4), because the length dl_{quad1} in (3) can be expressed with the length of an arc and the reluctance in (1) is linearly proportional to the length of flux path. In other words, the length dl_{quad1} can be expressed with the average length of arc between the point C and the point D. Therefore, the mean length of flux path dl_{quad1} gets to be $(X_1/2)d\theta_1$.

$$dl_{quad1} = \frac{X_1}{2} d\theta_1 \tag{4}$$

The cross section area S_{θ_1} for the infinitesimal element at θ_1 is the same as the area created by the revolution about y_1-axis of the line segment passing the two points $C(r_1, 0)$ and $D(r_1 + X_1 \cos\theta_1, X_1 \sin\theta_1)$. The area can be calculated by referring to [10]. Then the area S_{θ_1} is obtained as (5).

$$S_{\theta_1} = \int_0^{X_1 \sin\theta_1} 2\pi x_1 \sqrt{1 + \left(\frac{dx_1}{dy_1}\right)^2}\, dy_1 \tag{5}$$

The reluctance R_{quad1} for the quadrant is the integral of the reluctance for the infinitesimal element from $\theta_1 = 0$ to $\theta_1 = \pi/2$. Therefore, the reluctance R_{quad1} in (6) is obtained by substituting (4) and (5) into (3) and then integrating it as (6).

$$R_{quad1} = \int_{\theta_1=0}^{\theta_1=\pi/2} dR_{quad1} \tag{6}$$

The linear equation passing the points C and D in Fig. 1 can be expressed as (7).

$$y_1 = \tan\theta_1 (x_1 - r_1) \tag{7}$$

So dx_1/dy_1 in (5) is obtained as (8).

$$\frac{dx_1}{dy_1} = \frac{1}{\tan\theta_1} \tag{8}$$

The S_{θ_1} is obtained as (9) by substituting (7) and (8) into (5).

$$S_{\theta_1} = 2\pi\sqrt{1+\frac{1}{\tan^2\theta_1}}\left(\frac{X_1^2\sin^2\theta_1}{2\tan\theta_1} + X_1 r_1 \sin\theta_1\right) \tag{9}$$

Now substitute the mean length dl_{quad1} and the area S_{θ_1} obtained each from (4) and (9) into (3) and substitute (3) into (6). And then solve the definite integral of (6), the reluctance R_{quad1} of the quadrant is obtained. By the way, it is not easy to solve the definite integral of (6) analytically because of the form of (9). For that reason, in this paper the definite integral was solved by numerical integration using the Newton-Cotes Algorithm presented in [11].

In the rectangle of the fringing field in Fig. 1, the cross section of flux is uniform and the length of flux path is clear as g_1, so the reluctance R_{rect1} of the rectangle can be obtained as (10).

$$R_{rect1} = \frac{g_1}{\mu_0\pi\left((r_1+X_1)^2 - r_1^2\right)} \tag{10}$$

As mentioned before, the fringing field in Fig. 1 consists of two quadrants and a rectangle, so the reluctance $R_{frg\_axial\_out}$ of the fringing field is calculated as (11) with R_{quad1} and R_{rect1} obtained in (6) and (10) each.

$$R_{frg\_axial\_out} = 2R_{quad1} + R_{rect1} \tag{11}$$

It is shown in Fig. 2 the inner fringing field of axial air gap for an axisymmetric solenoid actuator. The fringing field consists of a quadrant and a rectangle. The X_2 determines the range of fringing field in the same as the outer fringing field.

The reluctance R_{quad2} calculation method of the quadrant in Fig. 2 is the same as it of the quadrant in Fig. 1. So, the reluctance R_{quad2} can be obtained by solving (12) using numerical integral.

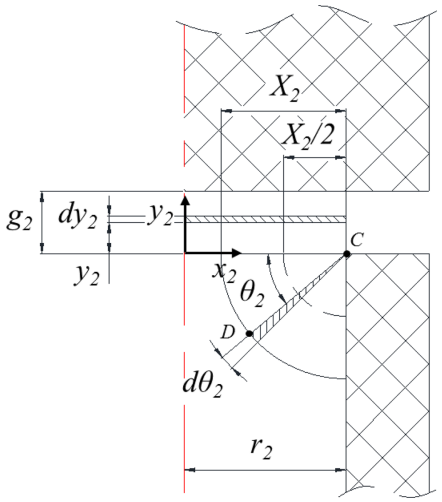

Fig. 2. (Color online) The inner fringing field of axial air gap.

$$R_{quad2} = \int_{\theta_2=0}^{\theta_2=\pi/2} dR_{quad2} \tag{12}$$

Merely, the area S_{θ_2} is calculated as (13) due to the different coordinate from Fig. 1.

$$S_{\theta_2} = 2\pi\sqrt{1+\frac{1}{\tan^2\theta_2}}\left(-\frac{X_2^2\sin^2\theta_2}{2\tan\theta_2} + X_2 r_2 \sin\theta_2\right) \tag{13}$$

In the same manner as the outer fringing field, the length dl_{quad2} can be expressed as (14).

$$dl_{quad2} = \frac{X_2}{2} d\theta_2 \tag{14}$$

Substituting (13) and (14) into (12) and solving (12) numerically give the reluctance R_{quad2} for the quadrant in Fig. 2. Similar to (10), The reluctance R_{rect2} for the rectangle in Fig. 2 is calculated as (15) from (1).

$$R_{rect2} = \frac{g_2}{\mu_0\pi\left(r_2^2 - (r_2 - X_2)^2\right)} \tag{15}$$

Thus, the reluctance $R_{frg\_axial\_in}$ of the fringing field in Fig. 2 is obtained as (16)

$$R_{frg\_axial\_in} = R_{quad2} + R_{rect2} \tag{16}$$

It is shown in Fig. 3 the fringing field of a radial air gap for an axisymmetric solenoid actuator. It is assumed that the fringing field consists of a quadrant and a rectangle, and the field positions symmetrically about the annular plate in up and down side each. In Fig. 3, only upper side is presented for avoiding complexity. And the X_3 determines the range of fringing field also here.

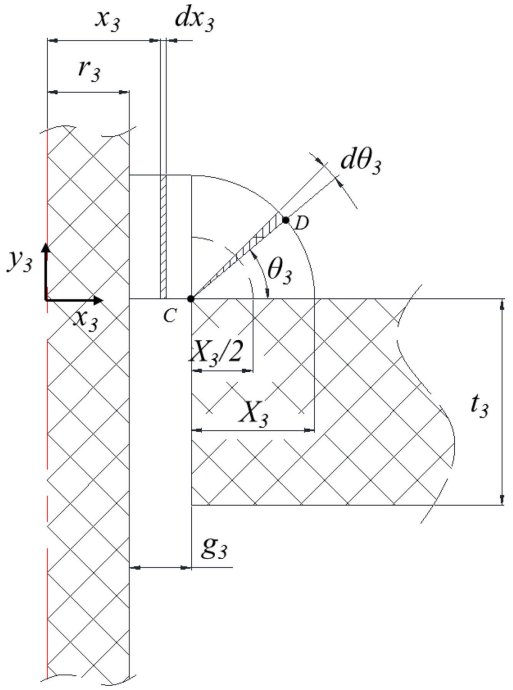

Fig. 3. (Color online) The fringing field of radial air gap.

The calculation method of reluctance R_{quad3} for the quadrant in Fig. 3 is the same as it of the quadrant in Fig. 1. So, the reluctance R_{quad3} can be obtained by solving (17) using numerical integral.

$$R_{quad3} = \int_{\theta_3=0}^{\theta_3=\pi/2} dR_{quad3} \tag{17}$$

The area S_{θ_3} with the dimensions presented in Fig. 3 is calculated in a similar manner to the outer fringing of axial air gap. Then the area S_{θ_3} is obtained as (18).

$$S_{\theta_3} = 2\pi\sqrt{1+\frac{1}{\tan^2\theta_3}}\left(\frac{X_3^2\sin^2\theta_3}{2\tan\theta_3}+X_3(r_3+g_3)\sin\theta_3\right) \tag{18}$$

The reluctance R_{rect3} for the rectangle in Fig. 3 can be calculated in the same way presented in [4] for the reluctance calculation of annular parts. Then, the reluctance R_{rect3} is obtained as (19).

$$\begin{aligned} R_{rect3} &= \int_{r_3}^{r_3+g_3}\frac{dx_3}{\mu_0 2\pi x_3 X_3} \\ &= \frac{1}{\mu_0 2\pi X_3}\ln\left(1+\frac{g_3}{r_3}\right) \end{aligned} \tag{19}$$

Because it has been assumed that the fringing field is symmetric about the annular plate, the reluctance R_{frg_radial} of fringing field near radial air gap is obtained by substituting (17) and (19) into (20).

$$R_{frg\_radial} = 2R_{quad3} + 2R_{rect3} \tag{20}$$

In using the circular-arc straight-line model, the determination of the range of fringing field is required such as X_1, X_2 and X_3. About ten times of air gap is mentioned in [9] but it should be determined considering shapes and dimensions of the objective model.

3. MEC Analysis for an Axisymmetric Solenoid Actuator

In the electronic controlled brake system for a vehicle, several solenoid valve actuators are applied for controlling wheel pressures and configuring hydraulic circuits for certain functions. A solenoid valve actuator among those kinds of solenoid valve actuators is shown in Fig. 4 [7] and it is Normally Open type (NO). The armature of NO solenoid valve actuator is enclosed by sleeve due to the feature of brake system that should be sealed completely. This sleeve for sealing should be non-ferromagnetic and it is arranged between the coil case and the armature in Fig. 4. That's why the solenoid valve actuators for electronic controlled brake system include not-ignorable radial gaps.

They are shown in Fig. 5(a) only the electromagnetically significant parts of solenoid actuators like Fig. 4. And the nodes in a view of magnetic equivalent circuit are shown together. The space occupied by sleeve in Fig. 4 is assumed as air and this space is regarded as a radial

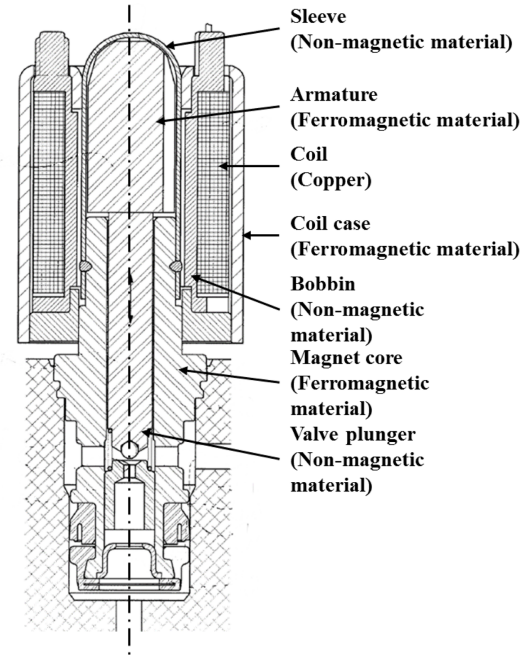

Fig. 4. A NO solenoid valve actuator of electronic controlled brake system.

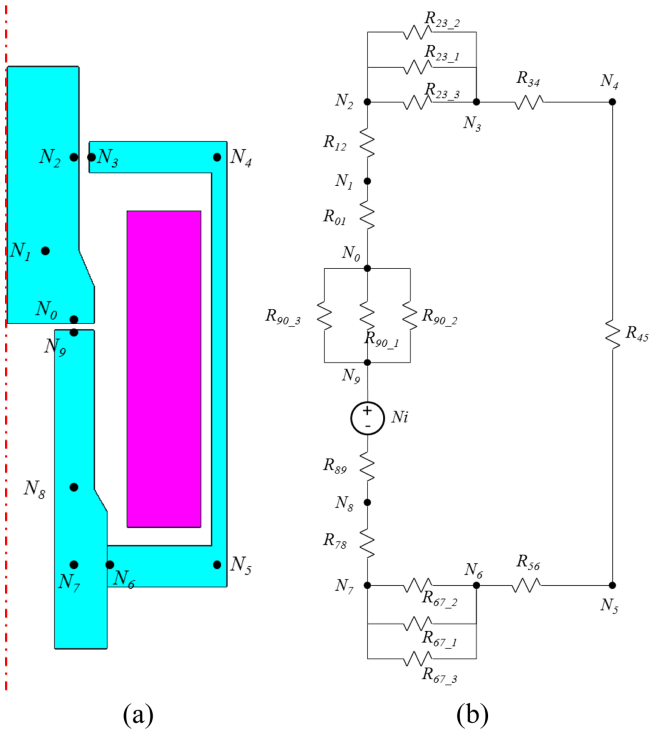

Fig. 5. (a) A cross section of axisymmetric solenoid actuator and MEC nodes (b) Magnetic equivalent circuit for the objective solenoid actuator.

air gap between the nodes N_2 and N_3 in Fig. 5(a). The attractive force in the axial air gap between the nodes N_0 and N_9 is valve closing force. Radial air gaps are there between the nodes N_2 and N_3 and the nodes N_6 and N_7. The radial air gap between the nodes N_2 and N_3 is larger than the axial air gap between the nodes N_0 and N_9. Thus, for a significant and accurate analysis result, the radial air gap should be included in MEC analysis of this solenoid actuator. As a result of MEC modeling for the solenoid actuator, the MEC model is shown in Fig. 5(b). Referring to [12], the coil arrangement wound around the axial air gap in Fig. 5 is minimizing leakage. And the solenoid valve actuators for brake systems are designed and taken into account the worst case on low voltage condition. For those reasons leakage flux was not considered in this paper.

In Fig. 5(b), the total reluctance R_{Total} of the MEC is calculated as (21).

$$R_{Total} = R_{90} + R_{01} + R_{12} + R_{23} + R_{34} + R_{45} + R_{56} + R_{78} + R_{89} \quad (21)$$

where,

R_{90}, R_{23}, R_{67} : the combined reluctances of air gaps and fringing fields

R_{01}, R_{12} : the reluctances of the solid and cylindrical shape parts consisting of ferromagnetic material

R_{34}, R_{56} : the reluctances of the annular and planar shape parts consisting of ferromagnetic material

R_{45}, R_{78}, R_{89} : the reluctances of the hollow and cylindrical shape parts consisting of ferromagnetic material.

The combined reluctance R_{90} is calculated as (22) for the three reluctances in parallel between the nodes N_0 and N_9.

$$R_{90} = \frac{R_{90\_1}R_{90\_2}R_{90\_3}}{R_{90\_1}R_{90\_2} + R_{90\_2}R_{90\_3} + R_{90\_3}R_{90\_1}} \quad (22)$$

where,

R_{90_1} : the reluctance of the axial air gap

R_{90_2} : the reluctance of outer fringing field near the axial air gap

R_{90_3} : the reluctance of inner fringing field near the axial air gap.

In the same manner, the reluctances R_{23} and R_{67} are calculated in (23) and (24) each.

$$R_{23} = \frac{R_{23\_1}R_{23\_2}R_{23\_3}}{R_{23\_1}R_{23\_2} + R_{23\_2}R_{23\_3} + R_{23\_3}R_{23\_1}} \quad (23)$$

$$R_{67} = \frac{R_{67\_1}R_{67\_2}R_{67\_3}}{R_{67\_1}R_{67\_2} + R_{67\_2}R_{67\_3} + R_{67\_3}R_{67\_1}} \quad (24)$$

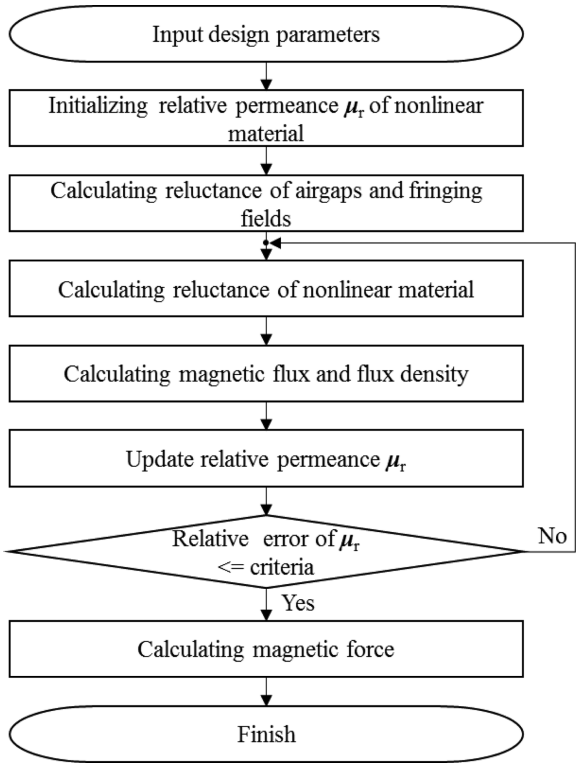

Fig. 6. Flow chart of MEC analysis using iterative method with B-H curves of nonlinear ferromagnetic material.

where,

R_{23_1}, R_{67_1} : the reluctances of radial air gaps
R_{23_2}, R_{23_3} : the reluctances of fringing fields near upper radial gap
R_{67_2}, R_{67_3} : the reluctances of fringing fields near lower radial gap.

The MEC in Fig. 5(b) is analyzed according to the procedure presented in Fig. 6. The procedure is similar to the procedures used in [3] and [4]. First set the initial relative permeances for the nonlinear material parts and calculate the reluctances of air gaps and fringing fields near them. Because air gaps and fringing fields have the constant permeability μ_0, one time calculation is enough. Hereafter, the iterative loop starts. Calculate the reluctances for nonlinear material parts and calculate fluxes and flux densities for all branches. And then update the relative permeances and make a judgement if all relative errors of the relative permeances satisfy pre-defined criteria. If the criteria satisfied for all branches, exit the loop and calculate a magnetic force, else the iteration goes on.

For MEC analysis, dimensions of the objective model shown in Fig. 5(a) are shown in Fig. 7 such as the lengths l between nodes, air gaps g and radii r.

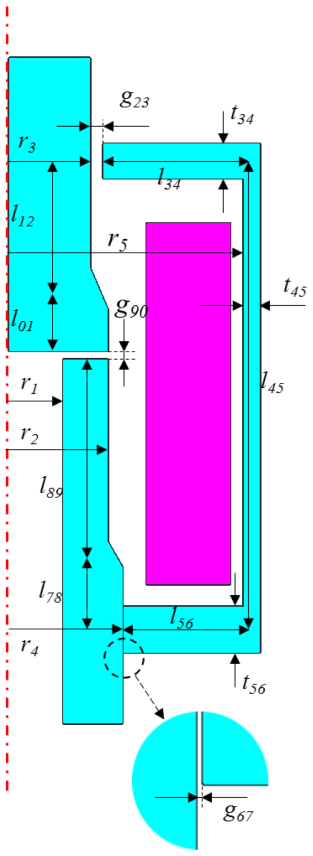

Fig. 7. (Color online) Dimensions of the objective solenoid actuator for MEC analysis.

The reluctance calculation step in the flow chart presented in Fig. 6 is done as follows. The reluctances of fringing fields such as R_{90_2}, R_{90_3}, R_{23_2}, R_{23_3}, R_{67_2}, R_{67_3} and of air gaps such as R_{90_1}, R_{23_1}, R_{67_1} are calculated in the introduced method above. i.e. they can be obtained by substituting the dimensions shown in Fig. 7 into the equations of the section 2 in this paper. For obtaining the reluctances of fringing fields such as R_{90_2}, R_{90_3}, R_{23_2}, R_{23_3}, R_{67_2} and R_{67_3}, it is required to determine the ranges of fringing fields corresponding X_1, X_2 and X_3 in Fig. 1, Fig. 2 and Fig. 3. And it is necessary to take account shapes and dimensions near fringing fields for the determinations. So, for the objective model presented in Fig. 7, ten times of the air gap g_{67} can be chosen as the ranges for R_{67_2} and R_{67_3} corresponding X_3 in Fig. 3, because the air gap g_{67} is small enough and there is no shape and dimension change in the ranges. And 5.5 times of the air gap g_{23} can be chosen as the ranges for R_{23_2} and R_{23_3} corresponding X_3 in Fig. 3, considering the length r_5-(r_3 + g_{23}) and the length l_{12}. More consideration is demanded in order to determine the ranges of fringing fields for R_{90_2} and R_{90_3} because they are effected by the radii r_2, r_5 and the length l_{01}. Additionally the fringing ranges for R_{90_2} and R_{90_3} corresponding X_1 in Fig. 1 and X_2 in Fig. 2 effect each other. Therefore, 2.5 times of the air gap g_{90} was chosen as the X_1 for R_{90_2} and the X_2 for R_{90_3} after some tries out. Next, the reluctances for the nonlinear ferromagnetic material parts and the airgaps are calculated in the traditional manner or the manner presented in [4] and [5]. The reluctances R_{01} and R_{12} of solid cylindrical shape parts are calculated as (25) and (26) each.

$$R_{01} = \frac{l_{01}}{\mu_r \mu_0 \pi r_2^{\,2}} \tag{25}$$

$$R_{12} = \frac{l_{12}}{\mu_r \mu_0 \pi r_3^{\,2}} \tag{26}$$

The μ_r is the relative permeability for ferromagnetic material. The reluctances of hollow cylindrical shape air gaps and ferromagnetic parts are obtained as (27)–(30).

$$R_{90\_1} = \frac{g_{90}}{\mu_0 \pi (r_2^{\,2} - r_1^{\,2})} \tag{27}$$

$$R_{89} = \frac{l_{89}}{\mu_r \mu_0 \pi (r_2^{\,2} - r_1^{\,2})} \tag{28}$$

$$R_{78} = \frac{l_{78}}{\mu_r \mu_0 \pi (r_4^{\,2} - r_1^{\,2})} \tag{29}$$

$$R_{45} = \frac{l_{45}}{\mu_r \mu_0 \pi ((r_5 + t_{45})^2 - r_5^{\,2})} \tag{30}$$

(25)–(30) are the results from substituting the cross section areas and the lengths of flux paths obtained from the dimensions shown in Fig. 7 into (1).

The reluctances of plate annular shape air gaps and ferromagnetic parts are obtained as (31)–(34) in the same manner presented in [4] and [5].

$$R_{23\_1} = \frac{1}{\mu_0 2\pi t_{34}} \log\left(\frac{r_3 + g_{23}}{r_3}\right) \tag{31}$$

$$R_{67\_1} = \frac{1}{\mu_0 2\pi t_{56}} \log\left(\frac{r_4 + g_{67}}{r_4}\right) \tag{32}$$

$$R_{34} = \frac{1}{\mu_r \mu_0 2\pi t_{34}} \log\left(\frac{l_{34}}{r_3 + g_{23}}\right) \tag{33}$$

$$R_{56} = \frac{1}{\mu_r \mu_0 2\pi t_{56}} \log\left(\frac{l_{56}}{r_4 + g_{67}}\right) \tag{34}$$

After the all reluctances are calculated and the criteria is satisfied by the iteration, the magnetic force can be calculated in (35) [6] with the flux density and cross section area at the node 9.

$$F_{mag} = \frac{B^2}{2\mu_0} S \tag{35}$$

The relation of flux density, flux and cross section area of flux path can be expressed as (36).

$$B = \frac{\Phi}{S} \tag{36}$$

Substituting (36) into (35) then, the magnetic force F_{mag} can be calculated from flux and cross section area as (37).

$$F_{mag} = \frac{1}{2\mu_0} \frac{\Phi^2}{S} \tag{37}$$

Therefore, the magnetic force F_{mag} of the objective model can be obtained in (38) from the fluxes Φ_{90_1} and Φ_{90_3}, and the areas S_{90_1} and S_{90_3} in the axial direction at node N_0.

$$F_{mag} = \frac{1}{2\mu_0}\left(\frac{\Phi_{90\_1}{}^2}{S_{90\_1}} + \frac{\Phi_{90\_3}{}^2}{S_{90\_1}}\right) \tag{38}$$

4. Comparison of MEC Analysis and FEA Result

The dimensions of the analyzed model are presented in Table 1. The material of the armature and the magnet core is S10C, and SPCC is applied to the coil case. In industry and practice, the armature and magnet core are manufactured by forging and the coil case is manufactured by pressing for cost reduction. Because the magnetic characteristics of these components are changed through such manufacturing process, customized B-H curves were applied in this paper.

Table 1. The dimensions of the analyzed model in accordance with Fig. 7.

Unit : mm

Parameters	Value	Parameters	Value	Parameters	Value
g_{90}	0.33	r_1	1.9	l_{12}	3.76
g_{23}	0.5	r_2	3.45	l_{34}	5.2
g_{67}	0.055	r_3	2.82	l_{45}	16.5
t_{34}	1.2	r_4	3.95	l_{56}	4.5
t_{45}	0.55	r_5	8.25	l_{78}	3.1
t_{56}	1.6	l_{01}	2.9	l_{89}	6.4

In case of electronic controlled brake system, because fail safety is critical point, so the performance and reliability on the worst case are taken into account during the design. Thus, solenoid actuators are designed taking account of the lowest voltage condition and generally the magnetomotive force (MMF) is around 500 [Ampere* Turns] on that condition. So, in this paper, MMF was changed around 500 [Ampere*Turns]. In Fig. 8, two results are compared, one is the result from the MEC analysis using the direct reluctance calculation method introduced in this paper and the other is obtained from FEA. In Fig. 8, it can be noticed that the result from the MEC analysis is similar to it from FEA.

And it is shown the relative error of the magnetic force and flux at the node N_0 with respect to FEA result in Table 2.

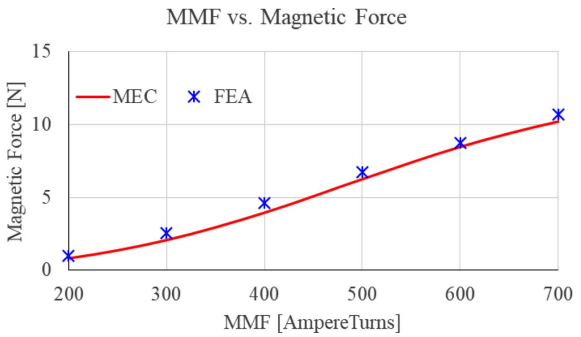

Fig. 8. (Color online) Magnetic force comparison of MEC analysis and FEA results.

Table 2. Relative error of MEC analysis result with respect to FEA result.

MMF (A*turns)	400	500	600	700
Flux error (%)	12.0	8.0	6.1	6.8
Force error (%)	14.6	6.8	3.0	4.4

From the comparison in Fig. 8 and Table 2, it can be noticed that the accuracy of MEC analysis using the introduced method is acceptable and the method directly calculating the reluctance of fringing field is valid.

As mentioned in the previous studies [4] and [5], MEC analysis can be used in optimization and dynamic simulation. Thus, for a validation of MEC analysis using the introduced method in a view of computation efficiency also, 4800 design cases were analyzed and a design was searched. The searched design satisfies defined constraints and consumes minimum current on the constraints. As design parameters, some dimensions presented in Fig. 7 such as r_2, t_{34}, t_{45}, t_{56} were selected. And coil parameters such as wire gage and the number of layers were chosen so that the number of combinations for the parameters became 4800. An optimization algorithm was not applied, just all cases are analyzed and filtered by constraints. For information, the computer specification used in the analysis was Intel Intel®Core™i5-2500K@3.30KHz, 16GB RAM and the CPU time for the 4800 cases was 17.57sec. And the program was coded in Fortran 95. The dimensions for the searched design is shown in Table 3.

In order to check the accuracy for the searched design also, the forces are compared between MEC analysis and FEA in Fig. 9.

Similar to the prior comparison result, it can be noticed that the force is resulted similarly between MEC analysis and FEA. Also the relative errors are shown in Table 4.

From Fig. 9 and Table 4, it can be noticed that the accuracy was maintained in the MEC analysis of the searched design. Therefore, considering the accuracy of MEC analysis using the direct reluctance calculation of fringing field and the computation efficiency, the introduced method in this paper can be utilized in MEC analysis for an axisymmetric solenoid actuator. Merely, in Table 4 the big difference between flux error and force error should be investigated additionally.

Table 3. The dimensions of the searched design.

Unit : mm

Parameters	Value	Parameters	Value	Parameters	Value
g_{90}	0.33	r_1	1.9	l_{12}	3.76
g_{23}	0.5	r_2	3.25	l_{34}	6.58
g_{67}	0.055	r_3	2.62	l_{45}	16.4
t_{34}	1.3	r_4	3.75	l_{56}	5.88
t_{45}	0.55	r_5	9.42	l_{78}	3.1
t_{56}	1.3	l_{01}	2.9	l_{89}	6.4

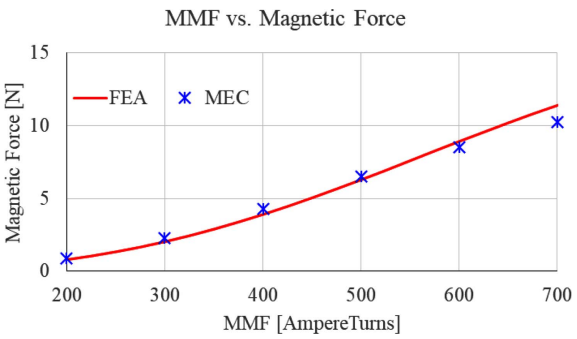

Fig. 9. (Color online) Magnetic force comparison of MEC analysis and FEA results for the searched design.

Table 4. Relative error of MEC analysis result with respect to FEA result for the searched design.

MMF (A*turns)	400	500	600	700
Flux error (%)	10.1	7.3	3.6	0.6
Force error (%)	8.9	3.3	4.5	11.2

5. Conclusion

In this paper, it has been introduced the method calculating directly the reluctances of fringing fields near radial air gaps as well as axial air gaps for an axisymmetric solenoid actuator. The calculation was facilitated by defining the infinitesimal element to be integrated in flux flowing direction. Using the calculation method, a MEC model for an axisymmetric solenoid actuator was analyzed and the result of MEC analysis was compared to the result of FEA. Through the comparison, it was proved that the MEC analysis using the introduced method has enough accuracy. And the computational efficiency of the MEC analysis using the method was shown by analyzing thousands of design cases in short time. Merely, because leakage fluxes are not considered in this paper, there is a possibility that the accuracy of MEC analysis can be improved more by considering leakage flux.

References

[1] Henry A. Rowland, Philosophical Magazine, Series 4, **46**, 140 (1873).
[2] Herbert C. Roters, Electromagnetic Devices, John Wiley & Sons (1941) pp 246.
[3] J. H. Sim, D. Y. Kim, S. I. Kim, and J. P. Hong, IEEE Trans. Magn. **53**, 6 (2017).
[4] J. Cale, S. D. Sudhoff, and Li-Quan Tan, IEEE Trans. Magn. **42**, 1 (2006).
[5] Mark A. Batdorff and John H. Lumkes, IEEE Trans. Magn. **45**, 8 (2009).
[6] John R. Brauer, Magnetic Actuators and Sensors, John Wiley & Sons Inc. (2006).
[7] C. J. Lee, Mando Corp., US 7,862,130 B2 (2011).

[8] Paul H. Schimpf, Int. J. on Recent Trends in Engineering and Technology **8**, 2 (2013).
[9] Duane Hanselman, Brushless Permanent Magnet Motor Design, The Writer's Collective (2003).
[10] George B. Thomas, Thomas' Calculation, 11th ed., Pearson Addison-Wesley (2004) Ch.6.
[11] Seteven C. Chapra and Raymond P. Candle, Numerical Method for Engineering with Programming and Software Application, 3rd ed., McGraw-Hill (1998) Ch. 22.
[12] T. A. Lipo, Introduction to AC Machine Design, Vol. 1, WisPERC UW-Madison (1996) pp 54-57.